Int. J. Environ. Sci. Technol. (2014) 11:785–794
DOI 10.1007/s13762-013-0261-9

ORIGINAL PAPER

Adsorption of roxarsone by iron (hydr)oxide-modified multiwalled carbon nanotubes from aqueous solution and its mechanisms

J. Hu · Z. Tong · G. Chen ·
X. Zhan · Z. Hu

Received: 11 October 2012 / Revised: 2 March 2013 / Accepted: 10 March 2013 / Published online: 18 April 2013

Abstract The adsorption of roxarsone by iron (hydr)oxide-modified multiwalled carbon nanotubes (MWCNTs) from aqueous solution and its mechanism were investigated. The amount of roxarsone adsorbed by modified MWCNTs is higher than MWCNTs at the same condition. The results show that the sorption isotherms are nonlinear, and can be well fitted according to the Freundlich and Polanyi–Manes models. The adsorption kinetics could be well described by pseudo-second-order model. Thermodynamic analysis shows that the adsorption of roxarsone on the adsorbents is an exothermic and spontaneous process. Desorption process had no obvious desorption hysteresis phenomenon. The FT-IR and XPS analysis confirmed the loading of iron ions on the MWCNTs, and revealed the involvement of carboxyl groups and iron ions on the adsorption of roxarsone.

Keywords Adsorption · Desorption · Iron hydroxide modification · Multiwalled carbon nanotubes (MWCNTs) · Roxarsone

Introduction

Arsenic contamination, one of the global environment issues, has posed a series of severe health problems (Polizzotto et al. 2008). Roxarsone (3-nitro-4-hydroxyphenylarsonic acid) is an organoarsenic and has been used widely in poultry industry to improve feed efficiency and to control coccidial intestinal parasites for decades (Jones 2007). Almost all of the roxarsone added in animal feed is excreted into the manure, which eventually enters into aquatic or terrestrial environment with washing and runoff, or land application of poultry litter (Jackson et al. 2006). Previous studies have shown that roxarsone is lastly degraded to inorganic arsenic, causing serious arsenic contamination in the environment (Cortinas et al. 2006; Jackson et al. 2006; Makris et al. 2008). Therefore, it is very important to remove roxarsone from roxarsone-contaminated wastewater for avoiding artificial arsenic contamination.

Due to the large specific surface areas and structural properties, carbon nanotubes (CNTs) have shown their potential to remove micro-contamination and as promising adsorbents in water and wastewater treatment (Ren et al. 2011). According to the layers involved, CNTs are divided into single-walled carbon nanotubes (SWCNTs) and multiwalled carbon nanotubes (MWCNTs). Because of the strong interactions between organic chemicals and CNTs, CNTs have been used to remove atrazine (Chen et al. 2008), 2,4,6-trichlorophenol (Chen et al. 2009), polycyclic aromatic hydrocarbons (Yang et al. 2006b), and phenanthrene (Wang et al. 2011). Roxarsone contains organic group and arsenic ion and it can be supposed that there are good interactions between CNTs and roxarsone.

Previous studies have revealed that iron (III) and sandy soil have high affinities toward arsenic ion (Chen et al. 2007; Mohan and Pittman 2007; Nagar et al. 2013). Lim et al. investigated the adsorption of organic arsenate (monomethyl-arsenate) onto a calcium alginate encapsulated magnetic sorbent, and noted that the –COOH and Fe–O groups in the sorbent are involved in the adsorption

J. Hu · Z. Tong · G. Chen · Z. Hu (✉)
Department of Civil Engineering, School of Civil Engineering,
Hefei University of Technology, Hefei 230009, China
e-mail: zhhu@hfut.edu.cn

X. Zhan
Department of Civil Engineering, National University of Ireland,
Galway, Ireland

process (Lim et al. 2009). The adsorption between organic chemicals and CNTs can be attributed to multiple interactions, such as π–π electron–donor–acceptor (EDA) interaction, specific adsorption to surface hydroxyl groups, and hydrophobic interaction, etc. (Pan and Xing 2008). The combination of CNTs and iron would take advantage of the strength of these two materials, enhancing the adsorption to roxarsone.

A series of researches have been carried out to remove inorganic arsenic from aqueous environmental systems (Daus et al. 2004; Deschamps et al. 2005; Jegadeesan et al. 2010), however, the studies reported on the removal of organic arsenic species are very limited (Lim et al. 2009; Hu et al. 2012), especially for roxarsone. The objective of this study is to investigate the adsorption and desorption processes of roxarsone by iron-modified MWCNTs and their possible mechanisms, which would provide a sound solution for the treatment of roxarsone and other organoarsenic-contaminated wastewater.

The research was carried out at Hefei University of Technology, Hefei, China from January to April in 2012.

Materials and methods

Materials

MWCNTs (Model L-MWCNT-1020, purity >95 %) with diameter 10–20 nm and length 5–15 µm were purchased from Nanotech Port Co., Shenzhen, China. Roxarsone (purity >99 %, Fig. 1) and all other chemicals used in this study were of analytical reagent grade.

Preparation of iron-modified MWCNTs

To preload iron onto MWCNTs, 8 g MWCNTs was stirred, respectively, with 200 mL of 0.05 and 0.2 mol L^{-1} $FeCl_3 \cdot 6H_2O$ in beaker for 24 h. Then MWCNTs were separated from the solution by centrifugation for 10 min at 10,000 rpm, and washed with deionized water until no reddish color or precipitate formed with addition of a few drops of 1:10 phenanthroline, which was used to indicate whether there was residual iron in the washings. Washed particles were dried at 80 °C in a hot air flow oven. The dried iron-modified MWCNTs with 0.05 mol L^{-1} $FeCl_3 \cdot 6H_2O$ treatment (M-Fe-A) and iron-modified MWCNTs with 0.2 mol L^{-1} $FeCl_3 \cdot 6H_2O$ treatment (M-Fe-B) were stored in a desiccator for adsorption test. The specific surface area (SSA) of MWCNTs is 167.48 m^2/g with the specific mesopore volume of 0.417 cm^3/g, and the specific surface area of modified MWCNTs is 146.39 m^2/g with the specific mesopore volume of 0.392 cm^3/g.

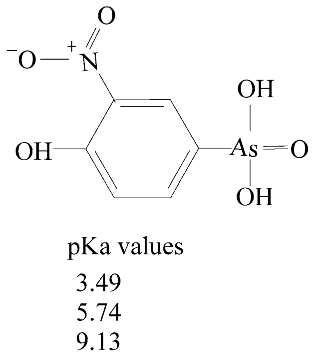

Fig. 1 Chemical structural formula of roxarsone

Adsorption and desorption experiments

Adsorption experiments were carried out using 100 mL flasks with working volume 50 mL. All adsorption tests were performed in triplicate. The flasks were stirred in a rotary shaker at 160 rpm. Samples were collected and centrifuged for 10 min to remove adsorbent. The supernatant was sampled for the determination of the residual roxarsone concentration. The pH values of the solutions were adjusted with 0.01 M HCl or 0.01 M NaOH.

To investigate the effect of pH on the adsorption process, the pH values ranging from 2.3 to 10.3 were used. The flasks containing 50 mL of 10.0 mg L^{-1} roxarsone and 0.2 g L^{-1} MWCNT or iron-modified MWCNT were shaken for 4 h. The temperature was controlled at 25 °C.

To investigate the thermodynamics of the adsorption process, three different temperatures of 288, 298, and 308 K were explored and the roxarsone concentrations were 5, 10, 20, 30, and 40 mg L^{-1}, respectively. Flasks containing 50 mL of 10.0 mg L^{-1} roxarsone and 0.2 g L^{-1} MWCNT or iron-modified MWCNT were shaken at pH 6.0 for 4 h.

To investigate desorption process, 0.1 g sorbent and 50 mL roxarsone solution were added to each flask. Three roxarsone concentrations of 10, 20 and 40 mg L^{-1} were used in the desorption experiment. The flasks were then shaken for 6 h at the temperature of 25 °C and pH 6.0, followed by settling for 30 min. An aliquot (25 mL) of supernatant was transferred to a clean vial for analysis. The flasks were refilled with 25 mL of the same roxarsone-free background solution to conduct another desorption cycle, and each sample was treated with four cycles. Desorption experiments were repeated three times.

Sample preparation for Fourier transform infrared and X-ray photoelectron analysis

Flasks containing 50 mL of 10.0 mg L^{-1} roxarsone and 0.2 g L^{-1} MWCNT or iron-modified MWCNT at pH 6.0

were shaken for 4 h to reach adsorption equilibrium. Supernatant was dumped carefully and the residues were transferred to vials for centrifuging. The roxarsone-loaded adsorbents were washed three times with deionized water to remove residual soluble roxarsone. The collected adsorbents were vacuum dried for Fourier transform infrared (FT-IR) and X-ray photoelectron spectroscopy (XPS) analysis.

Analysis

Roxarsone was determined by a LC-20 high performance liquid chromatography with a UV detector at wavelength 320 nm (Shimadzu Inc. Japan). A SHIM-PACK VP-ODS column (5 μm, 150 × 4.6 mm) (Shimadzu Inc. Japan) was used for the separation. The mobile phase was composed of 76 % 0.01 mol L^{-1} oxalic acid, 16 % acetonitrile and 8 % methanol, and the flow rate was 0.6 mL min^{-1}. The BET surface area was measured by ASAP 2020 Accelerated Surface Area and Porosimetry System (Micromeritics Instrument Corporation, USA). FT-IR analysis was carried out using a Magna-IR 750 (Nicolet Instrument Co., USA). Each sample for FT-IR analysis was mixed with pure potassium bromide and grounded in an agate mortar. The resulting mixture was pressed at 40 MPa for 5 min to form a uniform disk for analysis. The spectra were collected within the range of 400 and 4,000 cm^{-1}. All the spectra were recorded and plotted in the same scale on the transmittance axis. The surface composition of the adsorbents was analyzed by XPS spectra (Escalab 250Xi, Thermo Fisher Scientific, USA). For wide scan spectra, an energy range of 0–1,100 eV was used with pass energy of 40 eV and step size of 0.5 eV. The XPS spectra were collected in binding energy forms and fitted using a nonlinear least-squares curve fitting program (XPSPEAK41 software).

Results and discussion

Effects of pH

As shown in Fig. 2, adsorption capacity at same pH followed the order of M-Fe-B > M-Fe-A > virgin MWCNTs. The amount of roxarsone adsorbed on virgin MWCNTs, M-Fe-A, and M-Fe-B at equilibrium time showed a similar trend with pH changes, indicating that iron modification enhances the adsorption of roxarsone on MWCNTs. Taking M-Fe-B for example, the adsorption of roxarsone decreased quickly as the solution pH increased from 2.3 to 10.3. When the pH increased from 2.3 to 6.3, the amount of roxarsone adsorbed decreased significantly from 4.48 to 2.85 mg g^{-1}; while with the increase in pH from 6.3 to 8.5, the q_e was slightly affected by the variation of pH and the q_e decreased only from 2.85 to 2.77 mg g^{-1}. However, with further pH increase from 8.5 to 10.3, the q_e decreased significantly to 2.09 mg g^{-1}.

The variations of pH in solution, consequently, affect the adsorption characteristics for ionizable chemicals (Pan and Xing 2008). Roxarsone contains one benzene ring, one hydroxyl group, one nitro group, and one arsenic ion, as shown in Fig. 1, with pKa values of 3.49, 5.74, and 9.13, respectively (Qiang and Adams 2004). The variation of pH will change chemical speciation, hydrophilicity, and solubility of roxarsone in solution, and consequently affects the adsorption of roxarsone on the adsorbents. As shown in Fig. 2, at lower pH, there is a higher roxarsone adsorption, and the adsorption decreased with increasing pH, which is similar to the result of arsenic adsorption onto a magnetic sorbent (Lim et al. 2009). This might be because roxarsone are protonized, while MWCNTs are positively charged at low pH values, and electrostatic interactions become one of the dominant interaction forces (Zhang et al. 2010). With the increase of pH, the dissociation of roxarsone increased, which increases the solubility and hydrophilicity of roxarsone. The dissociated species of roxarsone also inhibit the formation of hydrogen bonds with MWCNTs (Wu et al. 2012). These make roxarsone adsorption unfavorable on MWCNTs with increasing pH.

Adsorption isotherms

Freundlich and Polanyi–Manes isotherms are widely used to describe the adsorption of organic chemicals on CNTs. The Freundlich isotherm is based on the adsorption phenomenon occurring on heterogeneous surface. Freundlich isotherm equation is given as:

$$q_e = K_f C_e^{\frac{1}{n}} \tag{1}$$

where K_f and n are Freundlich constants, C_e is equilibrium concentration of roxarsone in the solution (mg L^{-1}) and q_e

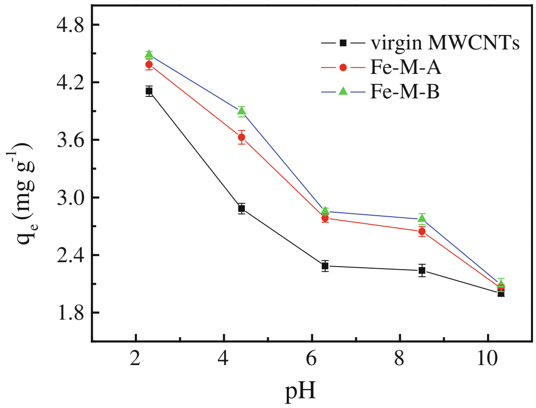

Fig. 2 Effect of pH on the adsorption of roxarsone by virgin MWCNTs and M-Fe-A and M-Fe-B

is the amount of roxarsone adsorbed by sorbent (mg g^{-1}) at equilibrium time. The equation can be linearized as:

$$\log q_e = \log K_f + \frac{1}{n} \log C_e \quad (2)$$

it is apparent that plots of log q_e against log C_e should yield straight lines and from which the values of K_f and n can be obtained.

The Polanyi theory has been widely employed for adsorption surfaces with heterogeneous energy distribution. The surface of CNTs generally consists of two energy states of carbon (graphite-like and disordered carbons). The Polanyi theory was developed to describe physical adsorption to microporous CNTs. This theory would appear to be applicable in this case since CNTs form bundles in aqueous media and the spaces between the tubes within the bundles can be regarded as pores (Pan and Xing 2008). The Polanyi–Manes model is given as:

$$q_e = Q^0 \exp(a(RT \ln(C_w/C_e))^b) \quad (3)$$

where Q^0 is the adsorption capacity, a and b are fitting parameters, R is the universal gas constant, T is the absolute temperature, and C_w stands for water solubility. In this study, the value of C_w is 500 mg L^{-1}.

The experimental data were fitted by Freundlich and Polanyi–Manes models (PMM), as shown in Fig. 3. Table 1 lists the adsorption parameters and the correlation coefficient values of roxarsone on MWCNT, M-Fe-A, and M-Fe-B with the two models. Freundlich model had a little higher correlation coefficient values for MWCNT, while PMM had a little higher correlation coefficient values for M-Fe-A and M-Fe-B, but all the correlation coefficient values are more than 0.985, which is in agreement with the results by Yang et al. (2006a). The result confirms that the adsorption sites are heterogeneous in energy distribution and the induced dipole-induced dipole force is the main force for the roxarsone adsorption on MWCNT and iron-modified MWCNT. High correlation coefficient values with PMM model in this case suggest that PMM seems not only applicable for pore filling but also applicable for surface adsorption. For all adsorbents, the adsorption capacity of roxarsone (Q^0) decreased with the increase of temperature, indicating that the adsorption of roxarsone was exothermic, which is further confirmed by thermodynamic analysis.

Adsorption kinetics

Adsorption kinetics is the most important character that provides insights into possible reaction mechanisms (Wu et al. 2012). A pseudo-second-order equation was used to fit the experimental data, which can be expressed as:

$$\frac{t}{q_t} = \frac{1}{K_2 q_e^2} + \frac{1}{q_e} t \quad (4)$$

where q_e and q_t are the amount of roxarsone adsorbed on adsorbent at equilibrium time and at time t, and K_2 is the rate constant. The values of q_e and K_2 can be calculated from the intercept and the slope of the linear plot of t/q_t versus t in Eq. (4).

Figure 4 (a, c, e) shows the effect of contact time on the adsorption of roxarsone by MWCNTs, M-Fe-A, and M-Fe-B with roxarsone concentrations of 10, 20, and 40 mg L^{-1}, respectively. For all adsorbents, adsorption uptake increased quickly in the first 1 h, and reached equilibrium gradually after 2–4 h depending on the concentrations of roxarsone. The high uptake at the start of the adsorption is due to the large amount of surface area available for adsorption. At this stage, the adsorption mainly occurred on the surface of the adsorbents. After the rapid uptake, the capacity of the adsorbent gradually became exhausted and the adsorption would be replaced by the transportation of roxarsone from the external sites to the internal pores of the adsorbent particles, which results in the dropdown of uptake rate.

Figure 4 (b, d, f) shows the fitting results of the data of Fig. 4 (a, c, e) with pseudo-second-order equation, while Table 2 lists the parameters obtained from the fittings. As seen in Table 2, the correlation coefficients were more than 0.99, indicating that the pseudo-second-order equation fitted very well to the adsorption process. Therefore, adsorption process of roxarsone by virgin MWCNTs and iron-modified MWCNTs could be described well using pseudo-second-order model, implying that a rate-controlling step of chemisorption promoted by covalent forces or valence forces was involved during the adsorption.

Thermodynamics analysis

Thermodynamics analysis will help to understand the adsorption mechanisms. In this study, the adsorption thermodynamics of roxarsone on virgin MWCNT, M-Fe-A, and M-Fe-B were analyzed at three different temperatures 288, 298, and 308 K with roxarsone concentration of 10.0 mg L^{-1}. Thermodynamic parameters were calculated using the following equations:

$$\Delta G^0 = -RT \ln K_c \quad (5)$$

$$K_c = \frac{C_s}{C_e} \quad (6)$$

$$\ln K_c = \frac{\Delta S^0}{R} - \frac{\Delta H^0}{RT} \quad (7)$$

where ΔG^0 represents standard free energy change, ΔH^0 represents standard enthalpy change, and ΔS^0 represents

Fig. 3 Adsorption isotherms of roxarsone on virgin MWCNTs, M-Fe-A and M-Fe-B at different temperatures fitted with Freundlich model (**a**, **c**, **e**) and Polanyi–Manes model (**b**, **d**, **f**)

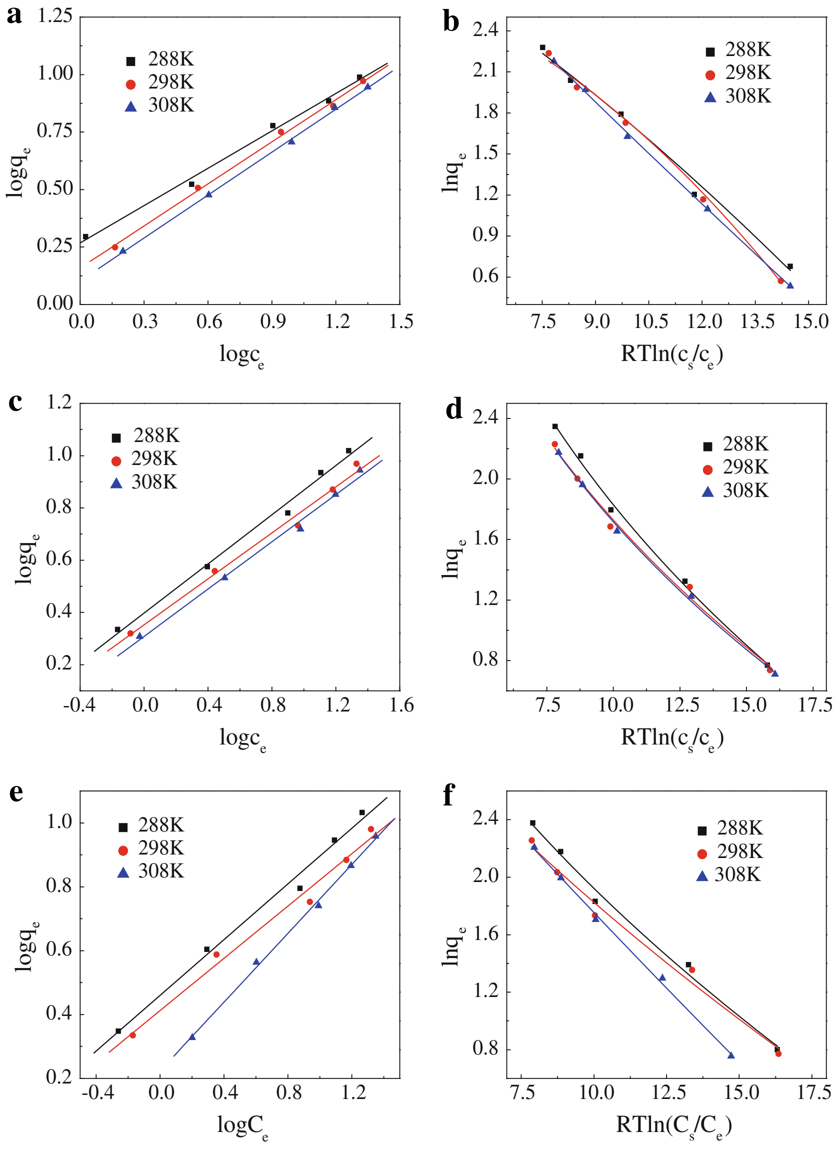

Table 1 Fitting of Freundlich model and PMM model to the adsorption of roxarsone on adsorbents at different temperatures

		Virgin MWCNTs			Fe–M–A			Fe–M–B		
		288 k	298 k	308 k	288 k	298 k	308 k	288 k	298 k	308 k
Freundlich	n	1.853	1.632	1.632	2.496	2.251	2.033	2.883	2.584	1.672
	K_f	1.833	1.543	1.312	2.126	2.274	2.210	2.444	1.856	1.856
	R^2	0.995	0.997	0.999	0.991	0.988	0.993	0.990	0.985	0.997
PMM	$\ln Q^0$	2.962	3.082	2.395	3.134	2.985	2.573	3.328	3.252	2.915
	a	−0.064	−0.013	−0.256	−1.679	−0.653	−0.335	−1.533	−0.553	−0.286
	b	1.425	1.856	0.895	0.644	0.713	0.954	0.503	0.672	0.911
	R^2	0.991	0.994	0.998	0.996	0.992	0.998	0.992	0.986	0.997

standard entropy change; K_c is the equilibrium constant, C_s is the equilibrium concentration of roxarsone on adsorbent (mg L^{-1}), and C_e is the equilibrium concentration of roxarsone in solution (mg L^{-1}), R is the ideal gas constant (8.314 J mol^{-1} K^{-1}), and T is the adsorption temperature in Kelvin.

Thermodynamics parameter values are listed in Table 3. The ΔG^0 values are in the range of −1.632 to −1.013,

Fig. 4 Adsorption kinetic of roxarsone on virgin MWCNTs (**a**), M-Fe-A (**b**), and M-Fe-B (**c**) at different concentrations and fitted with pseudo-second-order (**b**, **d**, **f**)

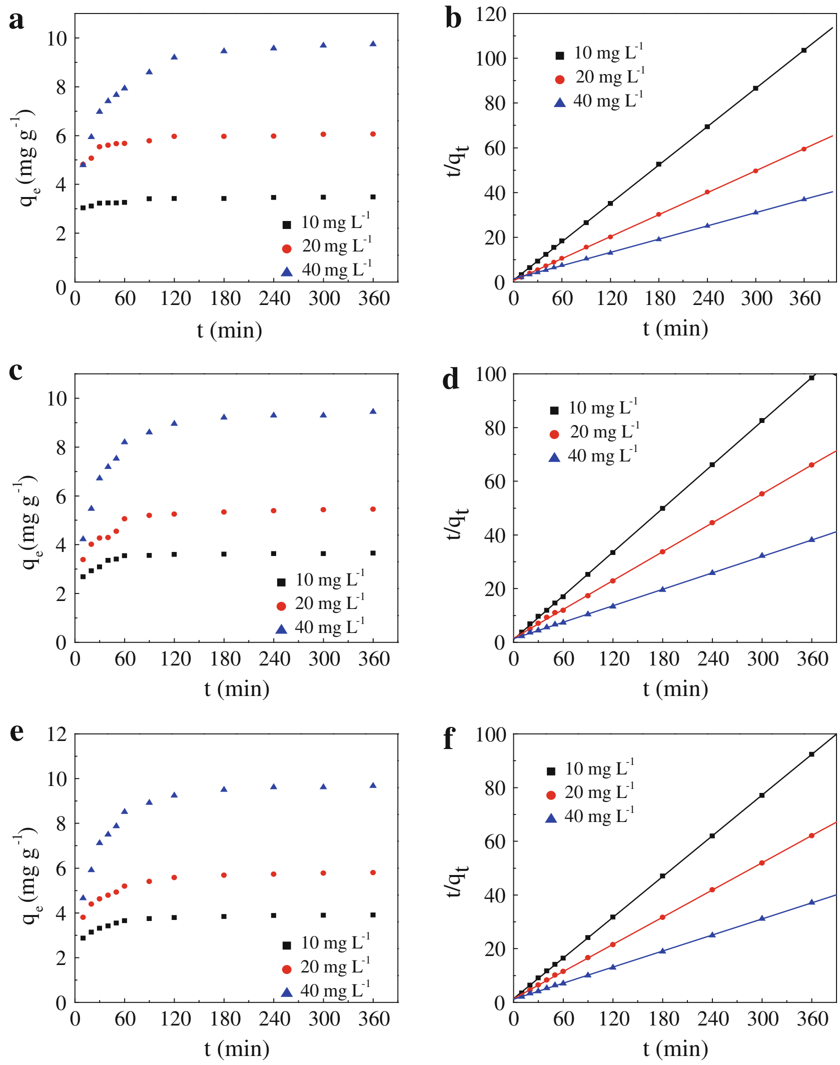

Table 2 Results of pseudo-second-order fitting to adsorption data of roxarsone on adsorbents at different initial concentrations (mg L^{-1})

	Virgin MWCNTs			M-Fe-A			M-Fe-B		
	10	20	40	10	20	40	10	20	40
K_2 g (mg^{-1} min^{-1})	0.093	0.048	0.007	0.047	0.021	0.008	0.065	0.021	0.007
q_e (mg g^{-1})	3.447	5.978	9.864	3.957	5.931	10.040	3.694	5.583	9.804
R^2	0.999	0.999	0.999	0.999	0.999	0.999	0.999	0.999	0.999

of −2.641 to −1.930 for M-Fe-A, and of −3.374 to −2.568 kJ mol^{-1} for M-Fe-B, which all are negative, indicating that the adsorption processes were exothermic and spontaneous. Therefore, the adsorption of roxarsone on the adsorbents was more favorable at a low temperature in the investigated temperature range. The negative value of ΔS^0 revealed a slight decrease in randomness at the solution interface with increasing temperature.

Desorption analysis

Figure 5 shows the adsorption and desorption isotherms of roxarsone on virgin MWCNTs, M-Fe-A, and M-Fe-B. There is no obvious desorption hysteresis during the desorption process. This might be attributed to the fact that MWCNTs are one dimensional hollow nano-size tubes and can easily adhere to each other to form

Table 3 Thermodynamic parameters for roxarsone adsorption on different adsorbents

	Virgin MWCNTs			M-Fe-A			M-Fe-B		
Temperature (k)	288	298	308	288	298	308	288	298	308
ΔG^0 (KJ mol^{-1})	−1.632	−1.429	−1.013	−2.641	−2.376	−1.930	−3.374	−3.058	−2.568
ΔH^0 (KJ mol^{-1})	−10.134			−12.847			−14.944		
ΔS^0(J K mol^{-1})	−0.031			−0.035			−0.040		

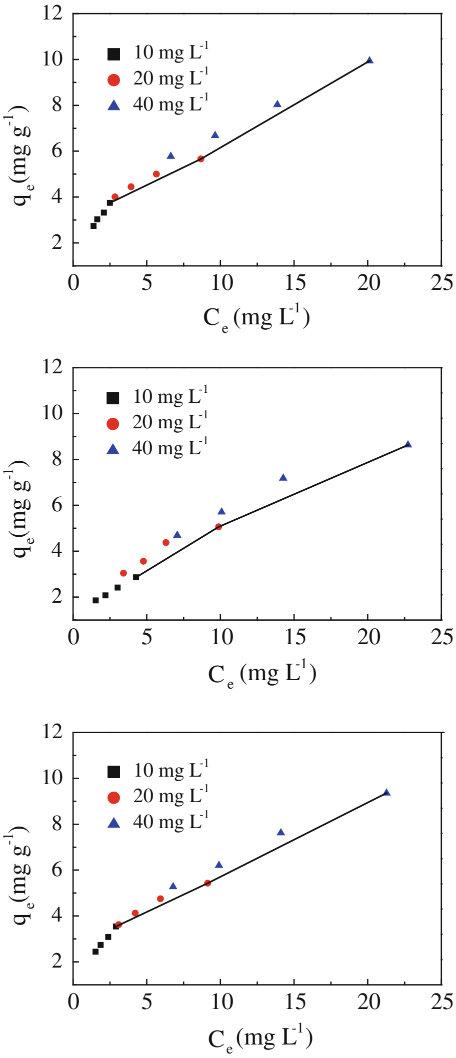

Fig. 5 Adsorption (*minus sign*) and desorption (*filled square*, *filled circle*, *filled triangle*) of roxarsone on virgin MWCNTs (**a**), M-Fe-A (**b**), and M-Fe-B (**c**) at different concentrations

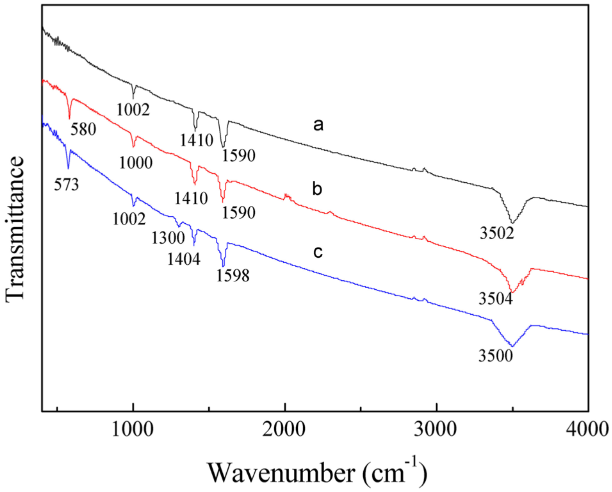

Fig. 6 FT-IR spectra for virgin MWCNTs (**a**), M-Fe-B(**b**), and roxarsone-loaded M-Fe-B(**c**)

aggregates due to strong van der Waals force interactions (Chen et al. 2008). However, Oleszczuk et al. reported the desorption hysteresis during the desorption process of oxytetracycline and carbamazepine on MWCNTs (Oleszczuk et al. 2009), indicating that desorption hysteresis is affected by the adsorbates and the environment. Usually, adsorption sites on bundles can be divided into four possible groups: outer surface sites of individual tubes and bundles, external groove sites, interstitial channels between nanotubes, interior of individual tubes (Chen et al. 2008). According to the performance of rapid adsorption and desorption process in this case, it can be deduced that the adsorption of roxarsone on modified MWCNTs mainly occurred on the outer surface of MWCNTs, which can explain the short equilibrium time during the adsorption process.

High adsorption capacity and reversible adsorption of roxarsone by iron-modified MWCNTs show that this material can be recycled as an adsorbent in water and wastewater treatments. However, the high adsorption capacity and no obvious desorption hysteresis also imply the high environmental risk, because the adsorption and desorption process affects the fate and toxicity of adsorbates in the environment (Hu et al. 2012). The easy desorption of roxarsone from environmental matrices could cause a real threat for the organisms when the desorbed roxarsone enters the environment (Oleszczuk et al. 2009).

Fig. 7 XPS spectra of adsorbents: (**a**) O1s of M-Fe-B; (**b**) O1s of roxarsone-loaded M-Fe-B; (**c**) C1s of M-Fe-B; (**d**) C1s of roxarsone-loaded M-Fe-B

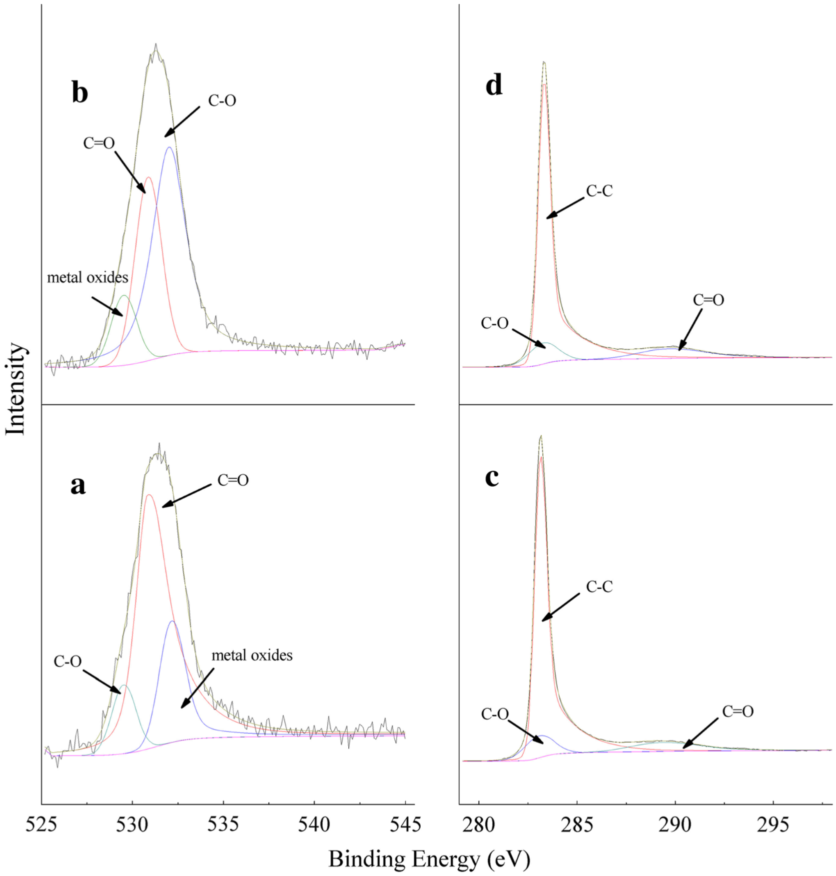

Table 4 Binding energy and relative content of O and C in adsorbents

Valence state	Sample	Proposed component	binding energy (eV)	area cps (eV)	Relative content (%)
O1s	M-Fe-B	Metal oxide (Fe–O, As–O)	529.5	1074.0	10.2
		C=O	530.8	7042.0	67.1
		C–O	532.2	2375.0	22.7
	roxarsone-loaded M-Fe-B	Metal oxide (Fe–O, As–O)	529.5	2293.2	11.5
		C=O	530.8	11335.9	56.8
		C–O	532.1	6319.8	31.7
C1s	M-Fe-B	C–C	283.2	158843.7	79.5
		C–O	283.4	20138.5	10.1
		C=O	289.5	19811.1	10.4
	roxarsone-loaded M-Fe-B	C–C	283.2	213499.1	78.9
		C–O	283.4	30040.9	11.3
		C=O	289.5	27243.8	9.8

FT-IR analysis

In order to investigate the possible adsorption mechanisms, virgin MWCNTs (sample a), M-Fe-B (sample b), and roxarsone-loaded M-Fe-B (sample c) were analyzed by FT-IR. The FT-IR spectra in Fig. 6 reveal the changes in the absorption bands of the surface functional groups of the adsorbents. In the virgin MWCNT, the bands at 3,502, 1,590, and 1,410 cm^{-1} are attributed to the O–H, C=O, and COO^{-1} stretching vibration, respectively (Lim et al. 2009). The spectra for virgin MWCNTs and M-Fe-B show that the absorption bands and shapes of the peaks are almost the same, except the appearance of a new peak at 580 cm^{-1}, which is assigned to the stretching vibration of Fe–O band, confirming the loading of iron ion on MWCNTs (Lim et al. 2008).

The spectra for M-Fe-B and roxarsone-loaded M-Fe-B show a minor shift in the frequencies of the absorption band of both C=O and C–O in carboxyl group (–COOH). The C=O bond shifts to the higher frequency from 1,590 to 1,598 cm^{-1}, which might be due to high electron density induced by the sorption of roxarsone onto the adjacent hydroxyl group (Lim et al. 2009). The C–O bond shifts from 1,410 to 1,404 cm^{-1}, which can be attributed to the associations of the hydroxyl group with roxarsone. The actions between modified MWCNTs and roxarsone might include π–π electron donor–acceptor (EDA) interaction, hydrogen bonding, van der Waals forces, and electrostatic interactions (Oleszczuk et al. 2009). The Fe–O bond also shifts to the lower frequency (from 580 to 573 cm^{-1}), which can be attributed to the associations of iron ions with roxarsone. These changes in bands indicate the carboxyl groups in the MWCNTs and modified iron ions are involved in the roxarsone uptake.

Because roxarsone contains three different arsenic chemical bonds As–C, As=O, and As–O, the appearance of an additional peak after adsorption at about 1,300 cm^{-1} (sample c) for As–C functional group shows an evidence of adsorption of roxarsone on the MWCNTs.

XPS analysis

Figure 7 shows the high resolution spectra of O1s and C1s regions of XPS spectra of iron hydroxide-modified MWCNTs and roxarsone-loaded MWCNTs. The O1s spectra can be deconvoluted into three peaks, representing three functional groups of metal oxides of Fe–O and As–O, C=O, and C–O, as shown in Fig. 7a–b. The peaks at binding energy of 529.5 eV can be assigned to the oxygen atom in the forms of metal oxides (Fe–O and As–O). The peaks with binding energies of 530.8 and 532.2 eV (for iron hydroxide-modified MWCNTs) and 530.8 and 532.1 eV (for roxarsone-loaded MWCNTs) can be assigned to the oxygen atom in the forms of C=O (carboxyl groups) and of C–O (ether groups), respectively (Lim et al. 2008), which reflects the main functional groups in the adsorbent.

The relative contents of O in different forms on the surface of the sorbents before and after adsorption are summarized in Table 4. It shows that the content of metal oxide groups of Fe–O and As–O increases from 10.2 to 11.5 % after the adsorption, indicating the appearance of As–O on the surface of modified MWCNTs. With the change of metal oxide after adsorption, the content of C–O groups increases from 22.7 to 31.7 %, while that of the C=O group decreases from 67.1 to 56.8 %. The results are contrast to the adsorption of copper adsorption onto an alginate encapsulated magnetic sorbent, which is because Cu^{2+} is a cation, while roxarsone is an anion in the solution (Lim et al. 2008). The changes in the contents of C–O and C=O indicate that they are involved in the adsorption of roxarsone onto the adsorbent, which is consonant with the result of FT-IR analysis, while the change of metal oxide groups confirmed the adsorption of roxarsone on MWCNTs.

As can be seen in Fig. 7c, d, the C1s spectra were deconvoluted into three peaks. These peaks can be assigned to the C atom in the forms of C–C, C–O (ether), and C=O (carboxyl) groups with binding energies of 284.5, 285.7, and 287.7 eV (for iron-modified MWCNTs and roxarsone-loaded MWCNTs). After adsorption of roxarsone, the quantity of C–O groups increases from 10.1 to 11.3 %, while that of the C=O group decreases from 10.4 to 9.8 %, which are consistent with the results from the O1s spectra analysis.

Conclusion

In this study, the adsorption and its mechanisms of roxarsone on virgin MWCNTs and iron-modified MWCNTs were investigated in aqueous system. Adsorption capacity at the same conditions was of the following order: iron-modified MWCNT with 0.2 mol L^{-1} $\text{FeCl}_3{\cdot}6\text{H}_2\text{O}$ treatment (M-Fe-B) > iron-modified MWCNTs with 0.05 mol L^{-1} $\text{FeCl}_3{\cdot}6\text{H}_2\text{O}$ treatment (M-Fe-A) > virgin MWCNTs. Freundlich and Polanyi–Manes models fitted very well with the adsorption of roxarsone on the adsorbents. Adsorption kinetics of roxarsone by the adsorbents could be better described in pseudo-second-order model. Desorption isotherm analysis shows that there is no obvious desorption hysteresis phenomenon. FT-IR analysis confirmed the loading of iron on the MWCNTs and reveals the involvement of carboxyl groups and iron ion on the adsorption of roxarsone. XPS analysis is consistent with the results of FT-IR analysis.

Acknowledgments This research was supported by the NSFC (51078122, 51108148), the NSFC-JST joint project (21021140001), Program for New Century Excellent Talents in University (NCET-11-0624), and the project-sponsored by SRF for ROCS, SEM (40th).

References

Chen W, Parette R, Zou J, Cannon FS, Dempsey BA (2007) Arsenic removal by iron-modified activated carbon. Water Res 41(9): 1851–1858

Chen GC, Shan XQ, Wang YS, Pei ZG, Shen XE, Wen B, Owens G (2008) Effects of copper, lead, and cadmium on the sorption and desorption of atrazine onto and from carbon nanotubes. Environ Sci Technol 42(22):8297–8302

Chen GC, Shan XQ, Wang YS, Wen B, Pei ZG, Xie YN, Liu T, Pignatello JJ (2009) Adsorption of 2,4,6-trichlorophenol by multi-walled carbon nanotubes as affected by Cu(II). Water Res 43(9):2409–2418

Cortinas I, Field JA, Kopplin M, Garbarino JR, Gandolfi AJ, Sierra-Alvarez R (2006) Anaerobic biotransformation of roxarsone and related *N*-substituted phenylarsonic acids. Environ Sci Technol 40(9):2951–2957

Daus B, Wennrich R, Weiss H (2004) Sorption materials for arsenic removal from water: a comparative study. Water Res 38(12): 2948–2954

Deschamps E, Ciminelli VST, Holl WH (2005) Removal of As(III) and As(V) from water using a natural Fe and Mn enriched sample. Water Res 39(20):5212–5220

Hu JL, Tong ZL, Hu ZH, Chen GW, Chen TH (2012) Adsorption of roxarsone from aqueous solution by multi-walled carbon nanotubes. J Colloid Interface Sci 377:355–361

Jackson BP, Seaman JC, Bertsch PM (2006) Fate of arsenic compounds in poultry litter upon land application. Chemosphere 65(11):2028–2034

Jegadeesan G, Al-Abed SR, Sundaram V, Choi H, Scheckel KG, Dionysiou DD (2010) Arsenic sorption on TiO(2) nanoparticles: size and crystallinity effects. Water Res 44(3):965–973

Jones FT (2007) A broad view of arsenic. Poult Sci 86(1):2–14

Lim S-F, Zheng Y-M, Zou S-W, Chen JP (2008) Characterization of copper adsorption onto an alginate encapsulated magnetic sorbent by a combined FT-IR, XPS and mathematical modeling study. Environ Sci Technol 42(7):2551–2556

Lim S-F, Zheng Y-M, Chen JP (2009) Organic arsenic adsorption onto a magnetic sorbent. Langmuir 25(9):4973–4978

Makris KC, Quazi M, Punamiya P, Sarkar D, Datta R (2008) Fate of arsenic in swine waste from concentrated animal feeding operations. J Environ Qual 37(4):1626–1633

Mohan D, Pittman CU Jr (2007) Arsenic removal from water/wastewater using adsorbents—a critical review. J Hazard Mater 142(1–2):1–53

Nagar R, Sarkar D, Makris KC, Datta R (2013) Inorganic arsenic sorption by drinking-water treatment residual-amended sandy soil: effect of soil solution chemistry. Int J Environ Sci Technol 10(1):1–10

Oleszczuk P, Pan B, Xing BS (2009) Adsorption and desorption of oxytetracycline and carbamazepine by multiwalled carbon nanotubes. Environ Sci Technol 43(24):9167–9173

Pan B, Xing BS (2008) Adsorption mechanisms of organic chemicals on carbon nanotubes. Environ Sci Technol 42(24):9005–9013

Polizzotto ML, Kocar BD, Benner SG, Sampson M, Fendorf S (2008) Near-surface wetland sediments as a source of arsenic release to ground water in Asia. Nature 454(7203):505-U5

Qiang ZM, Adams C (2004) Potentiometric determination of acid dissociation constants (pKa) for human and veterinary antibiotics. Water Res 38(12):2874–2890

Ren XM, Chen CL, Nagatsu M, Wang XK (2011) Carbon nanotubes as adsorbents in environmental pollution management: a review. Chem Eng J 170(2–3):395–410

Wang Z, Zhao J, Song L, Mashayekhi H, Chefetz B, Xing B (2011) Adsorption and desorption of phenanthrene on carbon nanotubes in simulated gastrointestinal fluids. Environ Sci Technol 45(14):6018–6024

Wu WH, Jiang W, Xia WX, Yang K, Xing BS (2012) Influence of pH and surface oxygen-containing groups on multiwalled carbon nanotubes on the transformation and adsorption of 1-naphthol. J Colloid Interface Sci 374:226–231

Yang K, Wang XL, Zhu LZ, Xing BS (2006a) Competitive sorption of pyrene, phenanthrene, and naphthalene on multiwalled carbon nanotubes. Environ Sci Technol 40(18):5804–5810

Yang K, Zhu LZ, Xing BS (2006b) Adsorption of polycyclic aromatic hydrocarbons by carbon nanomaterials. Environ Sci Technol 40(6):1855–1861

Zhang SJ, Shao T, Bekaroglu SSK, Karanfil T (2010) Adsorption of synthetic organic chemicals by carbon nanotubes: effects of background solution chemistry. Water Res 44(6):2067–2074